ISSN 0021-3640, JETP Letters, 2022, Vol. 116, No. 1, pp. 11–17. © The Author(s), 2022. This article is an open access publication, corrected publication 2022.
Russian Text © The Author(s), 2022, published in Pis'ma v Zhurnal Eksperimental'noi i Teoreticheskoi Fiziki, 2022, Vol. 116, No. 1, pp. 13–19.

FIELDS, PARTICLES, AND NUCLEI

New Constraints on the Axion–Electron Coupling Constant for Solar Axions

Yu. M. Gavrilyuk[a], A. N. Gangapshev[a], A. V. Derbin[b, *], I. S. Drachnev[b], V. V. Kazalov[a], V. V. Kuzminov[a], M. S. Mikulich[b], V. N. Muratova[b], D. A. Tekueva[a], E. V. Unzhakov[b], and S. P. Yakimenko[a]

[a] *Institute for Nuclear Research, Russian Academy of Sciences, Moscow, 117312 Russia*

[b] *Petersburg Nuclear Physics Institute, National Research Center Kurchatov Institute, Gatchina, Leningrad region, 188300 Russia*

**e-mail: derbin_av@pnpi.nrcki.ru*

Received May 25, 2022; revised May 25, 2022; accepted May 27, 2022

The resonant excitation of the ^{83}Kr first excited nuclear level ($E = 9.4$ keV) by solar axions whose fluxes depend on the axion–electron coupling constant g_{Ae} is sought. The γ- and X-ray photons and the conversion and Auger electrons from the excited-level relaxation are detected with a gas proportional counter of a low-background detector in the underground Baksan Neutrino Observatory (Institute for Nuclear Research, Russian Academy of Sciences). As a result, a new constraint $|g_{Ae}(g^3_{AN} - g^0_{AN})| \le 1.50 \times 10^{-17}$ (90% C.L.) has been obtained for the axion–electron and axion–nucleon coupling constants, which corresponds to new constraints on the axion mass $m_A \le 320$ eV and $m_A \le 4.6$ eV in the KSVZ and DFSZ axion models, respectively.

DOI: 10.1134/S0021364022601075

1. INTRODUCTION

Light pseudoscalar particles, axions, were introduced in the theory to solve the *CP* problem of strong interactions [1–3]. Despite negative results of intensive experimental searches for axions, they are still well-justified candidates for the dark-matter constituents [4]. The anomalous transparency of the Universe to high-energy γ rays [5] and the overly fast cooling of some star systems compared to the predictions of theoretical models [6] can be treated as promising astrophysical indications of the existence of axions.

The interaction of axions with matter is specified by the quantity f_A at which the Peccei–Quinn symmetry [1] is broken and is determined by the effective axion–photon ($g_{A\gamma}$), axion–electron (g_{Ae}), and axion–nucleon (g_{AN}) coupling constants. The axion mass m_A and the parameter f_A are related to the respective characteristics of the π^0 meson as $m_A f_A \approx m_\pi f_\pi$. The corresponding expression for m_A in terms of f_A has the form [7, 8]

$$m_A = 5.69(5)\left(\frac{10^6\ \text{GeV}}{f_A}\right)\text{eV}. \quad (1)$$

The original PQWW model of the "standard" axion [1–3] implies that PQ symmetry is broken at the electroweak scale $f_A = (\sqrt{2}G_F)^{-1/2} \simeq 250$ GeV. The constant f_A in two classes of new models KSVZ [9, 10] and DFSZ [11, 12] of the "invisible" axion can be arbitrarily large up to the Planck mass $m_P \sim 10^{19}$ GeV, thus reducing both the expected axion mass and the interaction of the axion with matter.

Stars should be intense sources of axions. Intense fluxes of axions can be formed in the Sun in a number of processes whose probabilities depend on the axion coupling constants $g_{A\gamma}$, g_{Ae}, and g_{AN}. The constant $g_{A\gamma}$ specifies the probability of conversion of photons to axions in the electromagnetic field of the solar plasma (Primakoff axions). The constant g_{AN} determines the emission of axions in nuclear magnetic transitions that are thermally excited at high temperatures in the center of the Sun or appear in nuclear reactions of the *pp* chain and CNO cycle. The constant g_{Ae} specifies the axion fluxes from bremsstrahlung $e + Z \to Z + e + A$ and Compton process $\gamma + e \to e + A$, as well as in discharge and recombination processes in atoms $I^* \to I + A$, $e + I \to I^* + A$. The spectra and fluxes of axions appearing in the above processes were calculated in [13–17] and are shown in Fig. 1.

Here, we report new results for the axion–electron coupling constant g_{Ae} determined from the complete set of data obtained in experiments on the search for the resonant absorption of solar axions by ^{83}Kr nuclei with a large krypton proportional counter [18, 19]. The

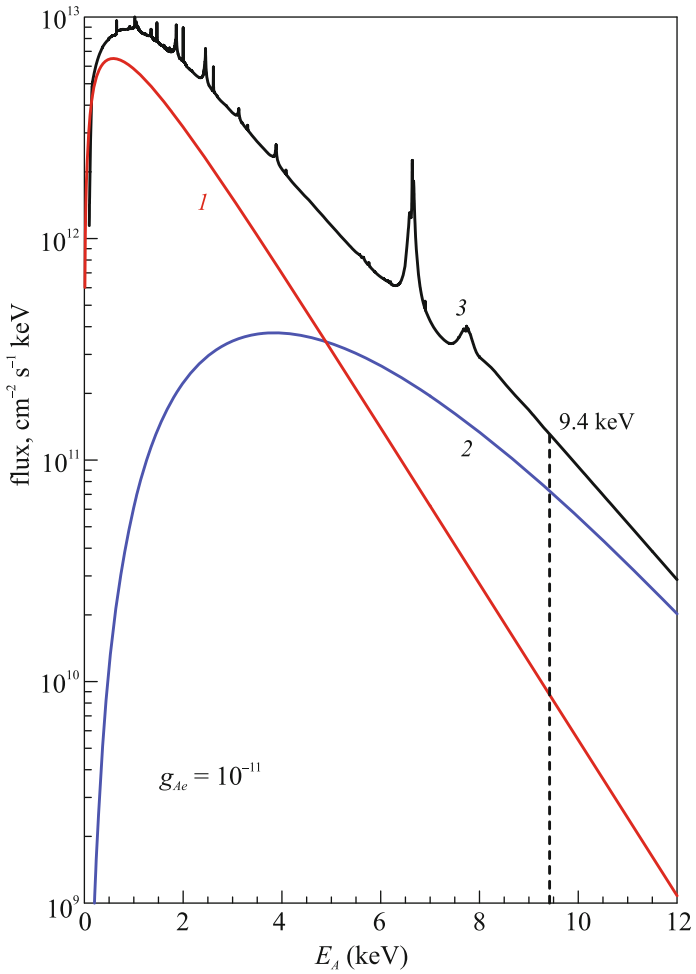

Fig. 1. (Color online) Energy spectrum of solar axions produced in (*1*) bremsstrahlung and (*2*) Compton processes and (*3*) sum of *1* and *2* including atomic processes as calculated with $g_{Ae} = 10^{-11}$.

cross section for the resonant excitation of a nuclear level depends on the constant g_{AN}; consequently, the rate of absorptions of axions in an experiment depends on the product of the constants g_{Ae} and g_{AN}.

The dimensionless coupling constant g_{Ae} in the DFSZ model is expressed in terms of the parameter f_A, which determines the axion mass m_A, and the free parameter $\cos^2\beta$:

$$g_{Ae} = (1/3)\cos^2\beta\, m_e/f_A, \qquad (2)$$

where m_e is the mass of the electron and β is an arbitrary angle. For the maximum value $\cos^2\beta = 1$ and taking into account Eq. (1), we obtain $g_{Ae} = 2.99 \times 10^{-11} m_A$, where m_A is in electronvolts.

In the KSVZ model, the axion does not interact with the electron; the effective axion–electron coupling constant calculated for the one-loop correction is [20, 21]

$$g_{Ae} = \frac{3\alpha^2 m_e}{4\pi^2 f_a}\left(\frac{E}{N}\ln\frac{f_A}{m_e} - \frac{2}{3}\frac{4+z+w}{1+z+w}\ln\frac{\Lambda}{m_e}\right), \qquad (3)$$

where $\alpha \approx 1/137$ is the fine-structure constant, $z = m_u/m_d = 0.56$ and $w = m_u/m_s = 0.029$ are the ratios of the masses of the u, d, and s quarks, $\Lambda \approx 1$ GeV is the scale cutoff in QCD, and E/N is the model-dependent parameter about unity, which is equal to 8/3 and 0 in the DFSZ axion model and the original KSVZ axion model, respectively. The interaction of the hadron axion with the electron is suppressed by a factor of at least $\sim\alpha^{-2}$.

According to Eqs. (2) and (3), the coupling constant g_{Ae} is proportional to m_A, with the coefficient of proportionality including unknown parameters $\cos^2\beta$ and E/N for the DFSZ and KSVZ axions, respectively. The axion coupling constants $g_{A\gamma}$, g_{Ae}, and g_{AN} determine both the probabilities of production of axions in various processes and cross sections for the reactions used to detect them.

The best known experiments are aimed at the search for solar axions produced through thermal-photon conversion in the field of the solar plasma. Under the assumption of the axion–photon coupling,

researchers attempt to detect axions through the inverse axion–photon conversion in a laboratory magnetic field [22, 23] or in a crystal field [24, 25]. Photon count rates expected in these experiments are proportional to $g_{A\gamma}^4$. In this work, to detect solar axions appearing in reactions involving the electron, the resonant absorption of axions by ^{83}Kr nuclei is employed. In this case, the expected count rate is proportional to the dimensionless product $g_{Ae}^2 \times g_{AN}^2$.

In our previous works, using a krypton proportional counter, we attempted to detect monochromatic solar axions emitted in the relaxation of the ^{83}Kr first excited nuclear level, which is excited because of the high temperature of the Sun [18], and Primakoff axions, which resonantly excite the ^{83}Kr nucleus [19]. Theoretical and experimental studies of the axion problem are reviewed in [8].

2. RESONANT EXCITATION OF THE ^{83}Kr FIRST EXCITED NUCLEAR LEVEL BY SOLAR AXIONS

Figure 1 shows the energy spectrum of axions produced in the processes caused by the axion–electron coupling that was calculated with the axion–electron coupling constant $g_{Ae} = 10^{-11}$ [17] and is used in further calculations. The average energy of axions is 1.6 keV and their flux almost vanishes at energies above 15 keV. The flux of axions at an energy of 9.4 keV, which corresponds to the ^{83}Kr first excited nuclear level, is 1.32×10^{11} cm^{-2} s^{-1} keV^{-1} [17], which is a factor of 60 lower than the maximum flux reached at an energy of 0.7 keV.

The 9.405-keV ^{83}Kr first excited nuclear level has the spin and parity $7/2^+$. The transition to the $9/2^+$ ground state is an $M1$ magnetic transition (a small fraction of the $E2$ transition is $\delta = 0.0129$) and can be accompanied by the emission of a γ-ray photon and by the emission or absorption of a pseudoscalar particle, an axion. The electron conversion coefficient important for target–detector experiments, where conversion and Auger electrons are absorbed in the target, is $e/\gamma = 17.1$ for the transition under study [26].

The ratio of the probabilities of the axion and electromagnetic transitions ω_A/ω_γ was calculated in the long-wavelength approximation in [27, 28] in the form

$$\frac{\omega_A}{\omega_\gamma} = \frac{1}{2\pi\alpha(1+\delta^2)}\left[\frac{g_{AN}^0\beta^* + g_{AN}^3}{(\mu_0 - 0.5)\beta^* + \mu_3 - \eta}\right]^2\left(\frac{p_A}{p_\gamma}\right)^3, \quad (4)$$

where p_γ and p_A are the momenta of the photon and axion, respectively; δ is the ratio of probabilities of the $E2$ and $M1$ transitions; $\mu_0 \approx 0.88$ and $\mu_3 \approx 4.71$ are the isoscalar and isovector nuclear magnetic moments, respectively; and β^* and η are the parameters determined by particular nuclear matrix elements. The parameters β^* and η for the $^{83}_{36}$Kr nucleus with an odd number of nucleons and an unpaired neutron are estimated in the single-particle approximation as $\beta^* = -1$ and $\eta = 0.5$ [29].

The axion–nucleon coupling constant g_{AN} is the sum of the isoscalar g_{AN}^0 and isovector g_{AN}^3 parts. In the KSVZ axion model, the constants g_{AN}^0 and g_{AN}^3 can be expressed in terms of the mass of the axion as [19]

$$\begin{aligned} g_{AN}^0 &= -4.03\times10^{-8}(m_A/1\text{ eV}),\\ g_{AN}^3 &= -2.75\times10^{-8}(m_A/1\text{ eV}). \end{aligned} \quad (5)$$

To calculate Eqs. (5), we used the particular axial vector baryon coupling constants $F = 0.462$ and $D = 0.808$ and the polarization structure function of the proton $S = 0.5$ [19], as well as the commonly accepted ratios $z = m_u/m_d = 0.56$ and $w = m_u/m_s = 0.029$ of the masses of the u, d, and s quarks (rather than more modern values $z = 0.47$ and $w = 0.023$ [8]) to correctly compare to the previous results.

We note that the detection of the resonant absorption of axions on the $M1$ transition in the ^{83}Kr nucleus is complicated by a methodological problem of a negative value of the parameter β^* in Eq. (4). This negative value, together with the existing wide interval of possible S and z values, leads to a large uncertainty of the ratio ω_A/ω_γ given by Eq. (4). The effect of uncertainties in the parameters S and z on the final result through a factor of $(g_{AN}^0 - g_{AN}^3)^2$ in Eq. (4) was discussed in [18, 19, 30], where it was shown in particular that the $(g_{AN}^0 - g_{AN}^3)^2$ value at the relation $S \simeq 1.2$–$1.7z$ can be more than an order of magnitude smaller than the value calculated with $S = 0.5$ and $z = 0.56$.

In the DFSZ axion model, the axion–nucleon coupling constants g_{AN}^0 and g_{AN}^3 depend on an additional unknown parameter $\cos^2\beta$, but they are of the same order of magnitude [20, 31]. At $\cos^2\beta = 1$, the parameter $|g_{AN}^0 - g_{AN}^3|$ appearing in Eq. (4) for the axion emission probability ω_A/ω_γ is a factor of 2.05 larger than this parameter for the KSVZ axion.

The cross section $\sigma(E_A)$ for axion absorption at the energy E_A is given by an expression similar to the cross section for the resonant absorption of γ-ray photons with the correction to the ratio ω_A/ω_γ. The total cross section for axion absorption can be obtained by integrating $\sigma(E_A)$ over the solar-axion spectrum $(d\Phi_A/dE_A)$ [30]. As a result, the rate of absorption of solar axions R_A by the ^{83}Kr nucleus is given by the expression

$$R_A = \pi\sigma_{0\gamma}\Gamma(d\Phi_A/dE_A)(\omega_A/\omega_\gamma), \quad (6)$$

where $\sigma_{0\gamma} = 1.22\times10^{-18}$ cm^2 is the maximum γ-ray absorption cross section and $\Gamma = 2.95\times10^{-12}$ keV is the width of the ^{83}Kr first excited nuclear level.

The flux of these axions is proportional to g_{Ae}^2, and the ratio ω_A/ω_γ depends on the parameter $(g_{AN}^3 - g_{AN}^0)^2$. The resulting expression for the rate of axion absorption R_A by the ^{83}Kr nucleus in units of inverse seconds per atom in terms of the coupling constant has the model-independent form

$$R_A = 2.15\times10^4 g_{Ae}^2(g_{AN}^3 - g_{AN}^0)^2(p_A/p_\gamma)^3. \quad (7)$$

Substituting Eqs. (5) for the constants g_{AN}^0 and g_{AN}^3 in terms of the axion mass m_A obtained in the KSVZ model, the axion absorption rate can be expressed in terms of g_{Ae} and m_A, the latter being measured in electronvolts,

$$R_A = 3.53\times10^{-12} g_{Ae}^2 m_A^2 (p_A/p_\gamma)^3. \quad (8)$$

The total number of detected axions depends on the number of ^{83}Kr nuclei in the target, measurement time, and detector efficiency. The probability of observing the 9.4-keV peak depends on the background level of the experimental setup.

3. EXPERIMENTAL SETUP

The experimental setup is described in detail in our previous works [18, 19]. Here, we present only the basic characteristics. A detector with a gas proportional counter is located in the low-background underground Baksan Neutrino Observatory (Institute for Nuclear Research, Russian Academy of Sciences) at a depth of 4900 mwe, where the muon flux is (2.6 ± 0.09) m^{-2} day^{-1}, which is lower than that on the ground by a factor of 5×10^6 [32].

The cylindrical copper counter has a total volume of 10.8 L. A gold-plated tungsten wire running along the counter axis serves as an anode. To exclude the influence of edge effects on charge collection, the anode diameter is increased, which limits the working volume of the chamber to 8.8 L. The counter is filled with krypton enriched to 99.9% in the ^{83}Kr isotope at a pressure of 1.8 bar. The mass of the ^{83}Kr isotope in the working volume of the counter is 58 g. The passive shield of the counter consists of sequential copper, lead, and polyethylene layers. A 12.5-MHz digitizer is used to measure the amplitude of the pulse, the duration of its rising edge, and the secondary photoemission pulse. The procedure of analysis of the pulse shape is described in [33, 34]. The detection efficiency for the γ-and X-ray photons, as well as Auger and conversion electrons, arising from the relaxation of the ^{83}Kr 9.4-MeV excited level as estimated through a Monte Carlo simulation with the Geant4 package is $\varepsilon = 0.825$ [19].

4. RESULTS

The measurements were carried out. The energy spectrum of the proportional gas counter signals detected over a live time of 776.6 day is shown in Fig. 2. The most intense peak observed in the spectrum is due to the X-ray K Cu lines ($K_{\alpha1} = 8.048$ keV, $K_{\alpha2} = 8.028$ keV, and $K_\beta = 8.905$ keV) from the copper frame of the counter.

The second peak observed at an energy of ~13.5 keV consists of several peaks with close energies. The long-lived ^{81}Kr isotope ($\tau = 3.3\times10^5$ yr) is formed from the stable ^{82}Kr and ^{80}Kr isotopes under the action of neutrons and decays through electron capture into the ^{81}Br ground state with a probability of 99.7%. The absorption of the characteristic X rays and Auger electrons from bromide in the sensitive volume of the detector is responsible for the 13.47-keV peak corresponding to the binding energy of the electron in the K shell of the Br atom. X-ray photons emitted by krypton ($K_{\alpha12} = 12.65$ keV) and bromine ($K_{\alpha12} = 11.92$ keV) beyond the sensitive volume of the gas chamber make an additional contribution to the broadened 13.5-keV peak.

The measured spectrum is approximated in the range of 4–20 keV by the sum of a continuous background and four Gaussian peaks. The function describing the continuous background is the sum of a constant component and an exponential function of the energy E:

$$S_{bkg}(E) = a + b\exp(-cE) + \sum_1^4 S_i G(E, E_i, \sigma_i), \quad (9)$$

where a, b, and c are varying parameters. Three Gaussians describe the known 8.04-keV $K_{\alpha12}$ Cu and 8.905-keV K_β Cu peaks and the wide 13.5-keV peak. The fourth Gaussian describes the 9.405-keV axion peak whose position and width are set to the parameters of the E_1 peak $K_{\alpha12}$ Cu.

The approximation of the energy spectrum in the range of 4–20 keV corresponding to $\chi^2 = 156.3/147$ and $P = 0.28$ is shown by the solid line in Fig. 2. The 9.4-keV "axion" peak is not manifested statistically. To establish an upper bound on the number of counts in the 9.4-keV peak, we used the standard method to determine the profile $\chi^2(S_4)$ and the probability function $P(\chi^2(S_4))$. The upper bound on the number of peak events thus determined is $S_{\lim} = 140$ for 90% C.L.

The determined upper bound on the number of events in the 9.4-keV peak provides bounds on the axion–electron coupling constant g_{Ae}, $g_{AN}^3 - g_{AN}^0$, and the axion mass m_A according to Eqs. (7) and (8). The expected number of detected axions is

$$S_A = R_A N_{^{83}\mathrm{Kr}} T \epsilon \le S_{\lim}, \quad (10)$$

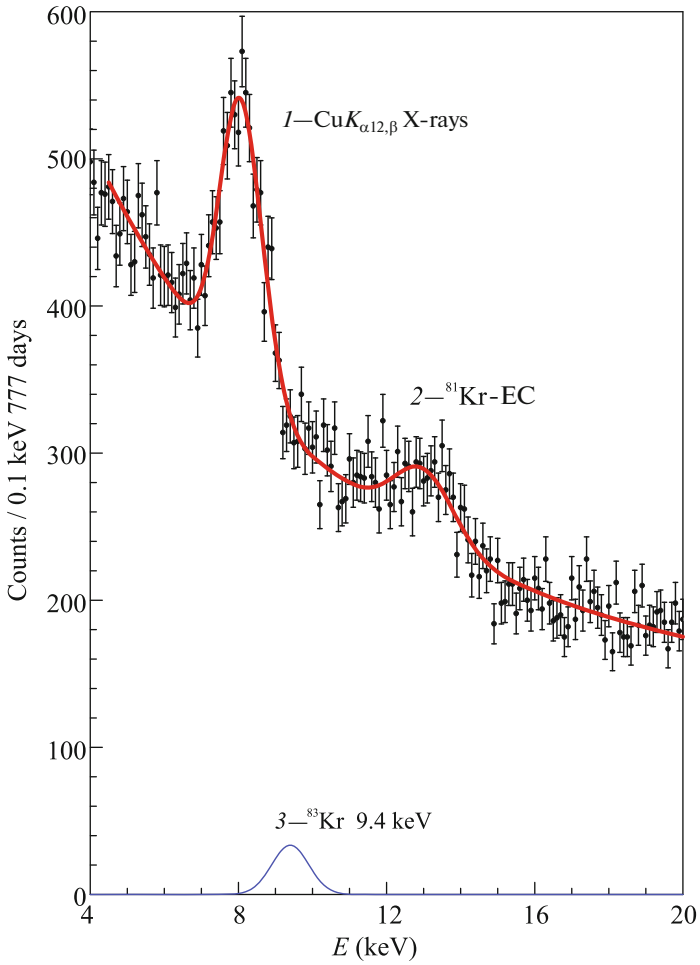

Fig. 2. (Color online) Spectrum of the proportional counter measured in 776.6 days and its theoretical approximations: (*1*) the Cu X-ray emission peak, (*2*) the peak from the ^{81}Kr decay and the Kr and Br X-ray emission, and (*3*) the 9.4-keV "axion" peak with the number of events $3S_{\text{lim}}$.

where $N_{83\text{Kr}} = 5.24\times10^{23}$ is the number of ^{83}Kr nuclei in the target, $T = 6.71\times10^{7}$ s is the measurement time, and $\epsilon = 0.825$ is the detection efficiency.

According to Eqs. (7) and (10), under the condition $(p_A/p_\gamma)^3 \cong 1$, which is valid for the masses of the axion $m_A < 2$ keV, we obtain the upper bound

$$|g_{Ae}(g^3_{AN} - g^0_{AN})| \le 1.50\times10^{-17} \qquad (11)$$

for 90% C.L. Bound (11) is a model-independent constraint on the coupling constants of the axion or any pseudoscalar axion-like particle to the electron and nucleon.

Using Eqs. (8) and (11), one can establish the following upper bound on the product of the constant g_{Ae} and mass m_A for the KSVZ axion:

$$|g_{Ae}\times m_A| \le 1.17\times10^{-9}\ \text{eV}. \qquad (12)$$

The upper bound (12) for the DFSZ axion at $\cos^2\beta = 1$ is almost two times lower $|g_{Ae}\times m_A| \le 5.72\times10^{-10}$ eV. The upper bound (12) on the allowed $|g_{Ae}\times m_A|$ values makes it possible to compare the results with the results of other experiments on the search for solar axions, in particular, with the results of the search for the axio-electric effect in atoms [36, 37] (Fig. 3).

The upper bound (12) excludes a new region of the coupling constant g_{Ae} at relatively large masses of the axion m_A and is a factor of almost 4 lower than the experimental result on the detection of resonant excitation of the ^{169}Tm first excited nuclear level [16, 35]. Since the 8.4-keV $M1$ transition in the ^{169}Tm nucleus is primarily a proton transition ($\beta \simeq 1$), the ratio ω_A/ω_γ does not include uncertainty.

Figure 3 shows the band of possible g_{Ae} and m_A values in the KSVZ and DFSZ axion models. Using Eqs. (2) and (3) for the axion–electron coupling constant, one can obtain upper bounds on the axion mass

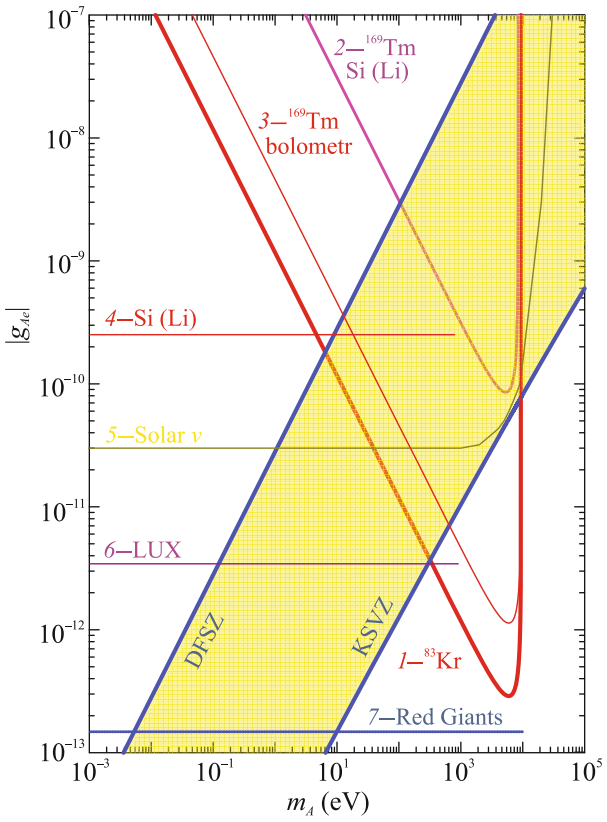

Fig. 3. (Color online) Upper bounds on the coupling constant g_{Ae} (line *1*) obtained in this work compared to the experimental results (*2*, *3*) on the resonant absorption of axions by the ^{169}Tm nucleus [16, 35], (*4*, *6*) on search for the axio-electric effect in (*4*) Si(Li) [36] and (*6*) LUX [37], (*5*) on the neutrino luminosity of the Sun [14], and (*7*) on astrophysical bounds [39]. The regions of excluded values lie above the corresponding lines.

in these two models from Eq. (12). The upper bound (12) on the product g_{Ae} and m_A excludes the axion masses $m_A > 320$ eV in the KSVZ model axion ($E/N = 8/3$). The upper bound on the DFSZ axion at $\cos^2\beta = 1$ and Eq. (2) is much lower: $m_A \le 4.6$ eV.

The upper bounds established in this work on the coupling constant of solar axions to the electrons for masses $m_A \ge 0.3$ keV are the most stringent laboratory constraints and are close to astrophysical constraints. It is interesting that the analysis of the luminosity of white dwarfs indicates a nonzero $|g_{Ae}|$ value in the interval of $(0.7–2.2) \times 10^{-13}$ [8, 38], although the corresponding upper bound is above the bound $|g_{Ae}| \le 1.3\times10^{-13}$ obtained for red giants in some globular clusters [39] (Fig. 3).

5. CONCLUSIONS

The resonant absorption of 9.4-keV solar axions by ^{83}Kr nuclei with the excitation of the first excited nuclear level has been sought. Gamma- and X-ray photons, as well as conversion and Auger electrons, have been detected with a large gas proportional counter that is filled with the ^{83}Kr isotope and is placed in a low-background detector in the underground Baksan Neutrino Observatory (Institute for Nuclear Research, Russian Academy of Sciences). As a result, a new upper bound $|g_{Ae}(g^3_{AN} - g^0_{AN})| \le 1.50 \times 10^{-17}$ (90% C.L.) has been obtained for the axion–electron and axion–nucleon coupling constants. This bound corresponds to constraints on the axion–electron coupling constant g_{Ae} and the axion mass m_A $|g_{Ae} \times m_A| \le 1.17\times10^{-9}$ eV and $|g_{Ae} \times m_A| \le 5.72\times 10^{-10}$ eV and on the axion mass $m_A \le 320$ eV and $m_A \le 4.6$ eV in the KSVZ and DFSZ ($\cos^2\beta = 1$) axion models, respectively.

FUNDING

This work was supported by the Russian Science Foundation (project no. 22-22-00017).

CONFLICT OF INTEREST

The authors declare that they have no conflicts of interest.

REFERENCES

1. R. D. Peccei and H. R. Quinn, Phys. Rev. Lett. **38**, 1440 (1977).
2. S. Weinberg, Phys. Rev. Lett. **40**, 223 (1978).
3. F. Wilczek, Phys. Rev. Lett. **40**, 279 (1978).
4. https://axion-wimp2021.desy.de.
5. S. V. Troitskii, JETP Lett. **105**, 55 (2017); arXiv: 1612.01864.
6. M. Giannotti, I. Irastorza, J. Redondo, and F. Ringwald, J. Cosmol. Astropart. Phys. **1605,** 057 (2016); arXiv: 1512.08108.
7. M. Gorghetto and G. Villadoro, J. High Energy Phys., No. 03, 033 (2019); arXiv: 1812.01008.

8. P. A. Zyla, R. M. Barnett, J. Beringer, et al. (Particle Data Group), Prog. Theor. Exp. Phys. **083C01,** 90 (2020).
9. J. E. Kim, Phys. Rev. Lett. **43**, 103 (1979).
10. M. Shifman, A. Vainshtein, and V. Zakharov, Nucl. Phys. B **166**, 493 (1980).
11. M. Dine, W. Fischler, and M. Srednicki, Phys. Lett. B **104**, 199 (1981).
12. A. Zhitnitskii, Sov. J. Nucl. Phys. **31**, 2 (1980).
13. L. M. Krauss, J. E. Moody, and F. Wilczek, Phys. Lett. B **144**, 391 (1984).
14. P. Gondolo and G. G. Raffelt, Phys. Rev. D **79**, 107301 (2009).
15. D. Kekez, A. Ljubičić, Z. Krečak, and M. Krčmar, Phys. Lett. B **671**, 345 (2009).
16. A. V. Derbin, A. S. Kayunov, V. V. Muratova, D. A. Semenov, and E. V. Unzhakov, Phys. Rev. D **83**, 023505 (2011).
17. J. Redondo, J. Cosmol. Astropart. Phys. **12**, 008 (2013).
18. Yu. M. Gavrilyuk, A. N. Gangapshev, A. V. Derbin, I. S. Drachnev, V. V. Kazalov, V. V. Kuz'minov, V. N. Muratova, S. I. Panasenko, S. S. Ratkevich, D. A. Semenov, D. A. Tekueva, E. V. Unzhakov, and S. P. Yakimenko, JETP Lett. **101**, 664 (2015).
19. Yu. M. Gavrilyuk, A. N. Gangapshev, A. V. Derbin, I. S. Drachnev, V. V. Kazalov, V. V. Kuzminov, V. N. Muratova, S. I. Panasenko, S. S. Ratkevich, D. A. Tekueva, E. V. Unzhakov, and S. P. Yakimenko, JETP Lett. **107**, 589 (2018).
20. M. Srednicki, Nucl. Phys. B **260**, 689 (1985).
21. S. Chang and K. Choi, Phys. Lett. B **316**, 51 (1993).
22. P. Sikivie, Phys. Rev. Lett. **51**, 1415 (1983).
23. V. Anastassopoulos, S. Aune, K. Barth, et al. (CAST Collab.), Nat. Phys. **13**, 584 (2017); arXiv: 1705.02290v2.
24. F. T. Avignone, D. Abriola, R. L. Brodzinski, et al., Nucl. Phys. Proc. Supll. **72**, 176 (1999).
25. E. Armengaud, Q. Arnaud, C. Augier, et al. (EDELWEISS Collab.), J. Cosmol. Astropart. Phys. **1311**, 067 (2013).
26. S. C. Wu, Nucl. Data Sheets **92**, 893 (2001).
27. T. W. Donnelly, S. J. Freedman, R. S. Lytel, R. D. Peccei, and M. Schwartz, Phys. Rev. D **18**, 1607 (1978).
28. F. T. Avignone, C. Baktash, W. C. Barker, F. P. Calaprice, R. W. Dunford, W. C. Haxton, D. Kahana, R. T. Kouzes, H. S. Miley, and D. M. Moltz, Phys. Rev. D **37**, 618 (1988).
29. W. C. Haxton and K. Y. Lee, Phys. Rev. Lett. **66**, 2557 (1991).
30. A. V. Derbin, S. V. Bakhlanov, A. I. Egorov, I. A. Mitropol'sky, V. N. Muratova, D. A. Semenov, and E. V. Unzhakov, Phys. Lett. B **678**, 181 (2009).
31. D. B. Kaplan, Nucl. Phys. B **260**, 215 (1985).
32. Yu. M. Gavriljuk, A. M. Gangapshev, A. M. Gezhaev, V. V. Kazalov, V. V. Kuzminov, S. I. Panasenko, S. S. Ratkevich, A. A. Smolnikov, and S. P. Yakimenko, Nucl. Instrum. Methods Phys. Res., Sect. A **729**, 576 (2013).
33. Yu. M. Gavrilyuk, A. M. Gangapshev, V. V. Kazalov, V. V. Kuz'minov, S. I. Panasenko, S. S. Ratkevich, and S. P. Yakimenko, Instr. Exp. Technol. **53**, 57 (2010).
34. Yu. M. Gavrilyuk, A. M. Gangapshev, V. V. Kazalov, V. V. Kuzminov, S. I. Panasenko, and S. S. Ratkevich, Phys. Rev. C **87**, 035501 (2013).
35. A. H. Abdelhameed, S. V. Bakhlanov, P. Bauer, et al., Eur. Phys. J. C **80**, 376 (2020).
36. A. V. Derbin, I. S. Drachnev, A. S. Kayunov, and V. N. Muratova, JETP Lett. **95**, 339 (2012).
37. D. S. Akerib, S. Alsum, C. Aquino, et al. (LUX Collab.), Phys. Rev. Lett. **118**, 261301 (2017).
38. M. M. Miller Bertolami, B. E. Melendez, L. G. Althausb, and J. Isern, J. Cosmol. Astropart. Phys. **1410**, 069 (2014).
39. F. Capozzi and G. Raffelt, Phys. Rev. D **102**, 083007 (2020).

Translated by R. Tyapaev